# Vortical Amplification of the Magnetic Field at an Inward Shock of Supernova Remnant Cassiopeia A

F. Fraschetti,[1,*] S. Katsuda,[2] T. Sato,[3] J. R. Jokipii,[4] and J. Giacalone[4]
[1]*Department of Planetary Sciences, University of Arizona, Tucson, Arizona 85721, USA;*
*Harvard/Smithsonian Center for Astrophysics, Cambridge, Massachusetts 02138, USA*
[2]*Graduate School of Science and Engineering, Saitama University, 255 Shimo-Ohkubo, Sakura, Saitama 338-8570, Japan*
[3]*RIKEN Nishina Center, 2-1 Hirosawa, Wako, Saitama 351-0198, Japan*
[4]*Departments of Planetary Sciences and Astronomy, University of Arizona, Tucson, Arizona 85721, USA*

(Received 24 January 2018; revised manuscript received 30 April 2018; published 21 June 2018)

We present an interpretation of the time variability of the x-ray flux recently reported from a multiepoch campaign of 15 years of observations of the supernova remnant Cassiopeia A by Chandra. We show for the first time quantitatively that the [4.2–6] keV nonthermal flux increase up to 50% traces the growth of the magnetic field due to a vortical amplification mechanism at a reflection inward shock colliding with inner overdensities. The fast synchrotron cooling as compared with shock-acceleration time scale qualitatively supports the flux decrease.

DOI: 10.1103/PhysRevLett.120.251101

Time variability of the x-ray flux of supernova remnants enables us to probe magnetohydrodynamic dynamo processes and particle acceleration at collisionless shocks [1]. Laboratory astrophysics experiments have identified a dynamo mechanism amplifying magnetic fields at shock waves [2]; however, direct astrophysical observations have been lacking.

A year-scale time variability in the x-ray filaments, or knots, of the supernova remnant Cassiopeia A was associated [3] with a fast synchrotron cooling in a strong magnetic field; a decline of the x-ray flux between 2000 and 2010 was observed with Chandra in the entire remnant's western limb [4]. Recent high spatial resolution multiepoch observations of Cassiopeia A have shown unprecedented evidence of an increase followed by a decrease of x-ray flux ([4.2–6] keV band) up to 50% in six distinct regions approximately $10 \times 10$ arcsec$^2$ or $15 \times 15$ arcsec$^2$ in size located on the west side and toward the center of the remnant [5]; such observations cover a period of 15 years (from 2000 to 2014). The location of those regions is consistent with a high-speed shock observed to move inward. Because of the young age of the remnant, such a shock is unlikely to correspond to the reverse shock, that would move outward at such an evolution stage, and plausibly originated as a reflection from the collision of the forward shock with an interstellar medium (ISM) molecular cloud; such a scenario was modeled in an earlier work [6]. As a result of such a reflection, the inward shock surface is likely to be corrugated to the scale of the molecular cloud.

In this Letter, we show for the first time that the overdensity clumps within the expanding plasma of Cassiopeia A, once crossed by the reflection inward shock, lead to the [4.2–6] keV flux increase via a magnetic field amplification through vorticity generation, as calculated by Fraschetti [7]. Such a process was first identified via two-dimensional magnetohydrodynamic (MHD) numerical simulations in Giacalone and Jokipii [8] and also investigated by several teams, including Inoue *et al.* [9].

Figure 1 is a cartoon illustration of the scenario envisaged: The corrugated inward shock travels through the

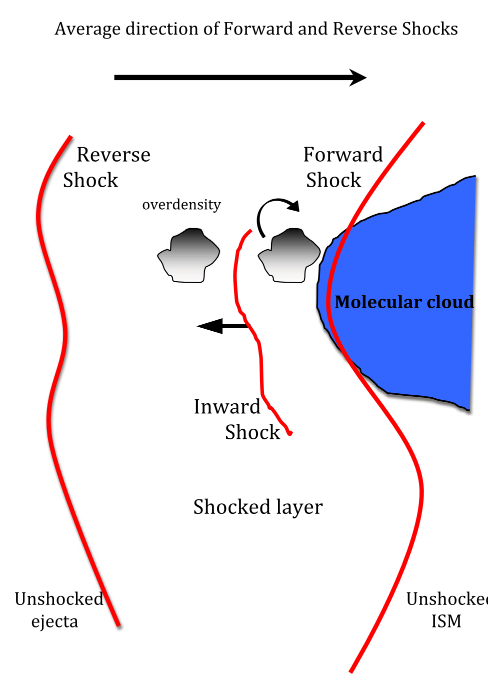


FIG. 1. Cartoon illustration of the proposed scenario: The inward shock recedes into the shocked layer and crosses the outward overdensity clumps thereby generating vorticity and the magnetic field enhancement in the downstream fluid. The arrows indicate the direction of the shocks' motion in the observer frame.

 

shocked layer, i.e., the hot plasma region between the forward and reverse shock, and therein collides with density clumps thereby generating vorticity and amplifying the magnetic field in the downstream fluid. The nonlinear field amplification is accounted for analytically within the MHD approximation [7]. The clumps might have originated in the supernova explosion itself (see, e.g., the 3D simulation in Müller *et al.* [10]) or from Rayleigh-Taylor instabilities triggered within the shocked layer as numerically determined in Refs. [11–13]. For the six regions within Cassiopeia A, the speeds of the inward shocks, if propagating into the shocked layer rest frame (Fig. 1), are inferred [5] to be in the range 5100–6800 km/s.

The time evolution of the turbulent amplified magnetic strength $B$ is determined analytically. The induction equation for $B$ is coupled with fluid equations to determine the MHD jump conditions at two-dimensional, i.e., corrugated, shock fronts; the vorticity generated behind the shock is related to $B$ via the small-scale dynamo process [14] leading to [from Fraschetti [7], Eq. (7) therein]

$$\left(\frac{B}{B_0}\right)^2(t) = \frac{e^{2t/\tau}}{1-\alpha\tau(1-e^{2t/\tau})v_A^2/2}, \qquad (1)$$

where $B_0$ is the upstream seed magnetic strength, and

$$\tau = \frac{r}{r-1}\frac{1}{C_r}\frac{R_c\ell_F}{R_c+\ell_F} \qquad (2)$$

is the growth time scale determined by the shock compression $r$, the curvature radius of the ripples on the forward shock surface $R_c$ that is expected to be comparable with the size of the overdensity clumps, the thickness of the outer clump layer where the density gradient is nonvanishing $\ell_F$ (corresponding to the field length in the ISM) and the shock speed in the upstream frame $C_r$. Here $\alpha \sim 1/R_cC_r$ describes the field backreaction to the whirling of the fluid, and $v_A$ is the seed field Alfvén speed. As calculated in detail in Ref. [7], the $B$ amplification occurs within the outer layer of thickness $\ell_F$.

In this Letter, we consider the region $W3$ only, according to the labeling in Ref. [5], which, along with the region W1, is least affected by thermal contamination, thereby allowing a better determination of the nonthermal flux. The flux increase in the other regions ($C1$, $C2$, $W1$, $W2$, $W4$) moving at speeds [5] different from $W3$ is arguably produced by the vortical amplification as well, with possibly different local best-fit values of $\ell_F$ and $R_c$ to be determined in a forthcoming work.

It is reasonable to assume that the nonthermal emission arises from synchrotron radiation of a population of energetic electrons in a strong and time-varying magnetic field $B(t)$. For simplicity, we assume that over a sufficiently small interval of electron Lorentz factor $\gamma = E/m_ec^2$ (where $m_ec^2$ is the electron rest energy), the differential energy distribution of the energetic electrons can be approximated with a simple power law: $dN/d\gamma = N_0(\gamma/\gamma_0)^{-p}$, where $\gamma_0$ is the injection electron Lorentz factor, and the index $p$ is determined by the shock compression only, as predicted by the linear test-particle version of the diffusive shock-acceleration model. It has been shown recently [15] that the baseline spectrum of the Crab nebula between radio and multi-TeV can result from a single log-parabola electron distribution, instead of commonly used multiple power laws. However, within the narrow photon energy range considered here ([4.2–6] keV), the emission spectrum from a log-parabola does not significantly depart from a power law; thus, we choose the latter as an acceptable approximation.

*Flux increase.*—The synchrotron power emitted by a single electron averaged over an isotropic electron distribution is given in the local plasma frame by $P(\gamma) = (\sigma_Tc/6\pi)\gamma^2B^2$, where $\sigma_T$ is the Thomson cross section, and $c$ is the speed of light in vacuum. The total synchrotron flux at Earth from a source at distance $d$, namely, $\nu F_\nu$, is found by folding $P_{\rm syn}$ with the differential energy distribution of the electrons: $\nu F_\nu = (1/4\pi d^2)\int d\gamma P_{\rm syn}N(\gamma)$. We use the monochromatic approximation; i.e., the electron power is concentrated around the characteristic synchrotron energy $\epsilon_s = 0.29(3eh\gamma^2B)/(4\pi m_ec)$, where $e$ is the electron charge, and $h$ is the Planck constant. Thus, the total flux observed at Earth, i.e., $\nu F_\nu \simeq (1/4\pi d^2)\times \int d\gamma P(\gamma)N(\gamma)|_{\epsilon=\epsilon_s}$, can be recast as

$$\nu F_\nu(\epsilon,t) = \frac{1}{4\pi d^2}\frac{\sigma_Tc}{12\pi}\frac{N_0}{\mathcal{A}}\gamma_0^p\epsilon^{-(p-3)/2}B(t)^{2+(p-3)/2}, \qquad (3)$$

where $\mathcal{A} = [0.29(3eh)/(4\pi m_ec)]^{-(p-3)/2}$ is a constant.

We reproduce in Fig. 2, upper panel, the observed flux change in the range [4.2–6] keV compared with the theoretical prediction [from Eq. (3)] for $\epsilon = 5$ keV, $d = 3.4$ kpc, and for distinct values of $R_c$. We emphasize that $C_r$, $B$, $\epsilon$, and $r$ (hence, $p$) are inferred from observations [5] and are not tuned here for data-fitting purposes. The model of the flux increase depends only on two fitting parameters, $R_c$ and $\ell_F$. The best-fit values for the time interval [2000∶2009] are

$$R_c = (1.00 \pm 0.16)\times 10^{18}\ \text{cm},$$
$$\ell_F = (7.03 \pm 0.76)\times 10^{17}\ \text{cm}. \qquad (4)$$

The error bars on $R_c$ and $\ell_F$ are likely dominated by the uncertainty on the exponential rise. In addition, the 2009 data point belongs to the incipient decrease phase of the flux; hence, it is not accounted for by our analytic model.

Figure 2, lower panel, depicts the amplification of the magnetic strength during the same time interval and for the same parameters as the upper panel. We show that the growth of $B$ extends beyond the flux maximum. However, this does not need to be the case, and the growth of $B$ might

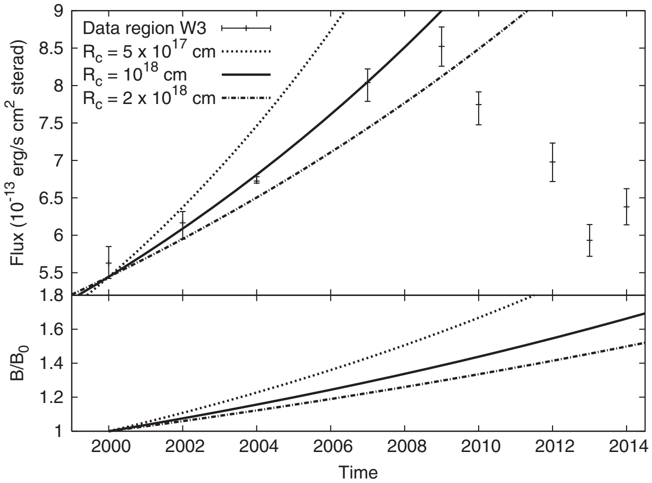


FIG. 2. Upper panel: Theoretical synchrotron flux at $\epsilon = 5$ keV as a function of time for distinct values of $R_c$ compared with Chandra [4.2–6] keV observations; here, $\ell_F = 7.03 \times 10^{17}$ cm. The best fit is represented by the solid line. Lower panel: Time evolution of relative magnetic strength during the turbulent amplification for the three cases shown above.

be hampered in the deep downstream medium. We do not consider in this short Letter such a possibility.

The Chandra observations of the x-ray flux increase [5] are consistent with a scenario of an inward shock traveling into a hot plasma with electron temperature ~2 keV (see, also, Ref. [16]), in equilibrium with ions: a low ion temperature is favored by the narrow lines in some bright knots within the remnant [17] despite not having been measured directly at the inward shock yet. For the W3 inward shock, $C_r = 6500$ km/s in the shocked layer frame, as derived [5] (Table 3) from the proper motion speed $3540 \pm 440$ km/s added to an expansion velocity ~3000 km/s. Thus, for a monoatomic gas, $r \sim 3.8$ leading to $p = 2.07$.

The best-fit values in Eq. (4) are compatible with previously reported observations. The linear size of the W3 box (~10 arcsec) capturing only the x-ray bright fraction of the extent of the inward shock where the $B$ field is amplified ($\ell_F$) corresponds to $\sim 5 \times 10^{17}$ cm at distance $d$. Such a size is in good agreement with the best-fit $\ell_F$ and is consistently smaller than the best-fit $R_c$ [Eq. (4)]. For the ISM, $\ell_F$ is not strongly constrained by thermal equilibrium models [18]. However, our best-fit $\ell_F$ is consistent with expectations from thermal conduction models in multiphase media, (see Ref [19], Eq. (5.1) and Sec. V (b) therein].

We note that the Chandra observations set an upper limit of the seed field $B_0$ since the year 2000; in other words, the amplification and the consequent flux increase are likely to have begun prior to 2000 by the same mechanism from a smaller $B_0$, although high-resolution observations of previous epochs are not available. Our best fit yields a growth time scale [Eq. (2)] $\tau^* \simeq 29$ yr, whereas the Chandra observations captured only approximately 9 years of the flux increase (from 2000 to 2009). We note that $\tau^*$ is appreciably longer than the time scale variation of x-ray brightness in the extreme cases previously reported, e.g., RX J1713.7–3946 from Uchiyama *et al.* [20] or in cases of very high Mach number shocks [7].

*Flux decrease.*—As an approximate marker of the $\nu F_\nu^{[4.2\text{–}6]\ \mathrm{keV}}$ peak occurring in approximately 2009 for W3, we can use the ratio of the synchrotron cooling time scale $t_{\mathrm{cool}}$ to the acceleration time scale $t_{\mathrm{acc}}$. By using a reference value for Cassiopeia A, $B_{0.1} = 5$, where $B_{0.1} = B/0.1$ mG, Sato *et al.* [5] find $t_{\mathrm{cool}} \simeq 4$ yr for the region W3. For an electron of Lorentz factor $\gamma$ emitting synchrotron power $P(\gamma)$ at a typical photon energy $\epsilon$ in an ambient downstream magnetic field $B$, we have

$$t_{\mathrm{cool}}(t) \simeq (55\ \mathrm{yr})\epsilon_{\mathrm{keV}}^{-1/2} B_{0.1}(t)^{-3/2}, \tag{5}$$

where $\epsilon_{\mathrm{keV}} = \epsilon/1$ keV and $B_{0.1}(t) = B(t)/0.1$ mG. Equation (5) is equivalent to Eq. (5) in Ref [5], where $B$ is taken as constant, with $\epsilon_{\mathrm{keV}} = 1.9 \times 10^{-3} (E_{\mathrm{TeV}})^2 B_{0.1}$ ($E_{\mathrm{TeV}}$ being the electron energy in TeV and the typical value of $E_{\mathrm{TeV}}$ is consistent with the value of $\gamma_0$ chosen here).

At $\epsilon_{\mathrm{keV}} = 5$, the value $t_{\mathrm{cool}} = 4$ yr yields at a time $t^\star = 2009$ the field $B_{0.1}(t^\star) \simeq 3.4$ in the expected range for Cassiopeia A, as discussed in Ref. [3]. The best-fit $B$ field (solid line in the lower panel in Fig. 2) shows a ratio $B(t^\star)/B_0 \simeq 1.35$ that leads to $B_{0(0.1)} = 2.5$, with $B_{0(0.1)} = B_0/0.1$ mG. Such a relatively high $B_0$ confirms that an amplification in W3 likely took place at the inward shock prior to the year 2000, possibly via vorticity generation within the shocked layer due to the corrugation of the inward shock or an alternative mechanism.

The acceleration time scale $t_{\mathrm{acc}}$ can be approximated by [21]

$$t_{\mathrm{acc}} \simeq 1.83 \frac{3r^2}{r-1} \frac{D_0}{C_r^2} = (43.7\ \mathrm{yr}) \frac{3r^2}{r-1} k_0 \epsilon_{\mathrm{keV}}^{1/2} B_{0.1}^{\prime -3/2} C_{r,3}^{-2}, \tag{6}$$

where for an isotropic upstream turbulence, $D_0$ is the diffusion coefficient at the electron cutoff energy and is along the average direction of shock motion, and $k_0$ assumed [21] to be equal upstream and downstream is given by $k_0 = D_0/D_B$, where $D_B$ is the Bohm diffusion coefficient at that energy. The departure from unity of $k_0$, both $k_0 > 1$ ($k_0 < 1$) for shocks close to quasiparallel (or quasiperpendicular) topology within the acceleration region indicates that the turbulence is not dominant over the seed field [22]. Finally, the upstream field, constant in time as the amplification occurs downstream in the model presented here for the flux increase (plasma kinetic instabilities are neglected), is given by $B'_{0.1} = B'/0.1$ mG and $C_{r,3} = C_r/(1000$ km/s). We note that Eq. (6) is equivalent to Eq. (6) in Ref. [5] with $B'_{0.1} = B_{0.1}(t) =$ const. For the current speed $C_{r,3} = 6, 5$ in region W3, we estimate $k_0 = 4.7$ from Eq. (3) in Ref [5]; for $B'_{0.1} = 2.5$, Eq. (6) provides at present $t_{\mathrm{acc}} \sim 42$ yr, significantly greater than $t_{\mathrm{cool}} \sim 4$ yr. A cooling faster than the acceleration [23] is consistent with the observed flux decrease. More sophisticated models for the diffusion coefficient (e.g., Refs. [24,25]) will not substantially change this qualitative argument; see next section.

We emphasize that $t_{\rm cool}(t)$ is time variable unlike what is customarily assumed: it shortens as $B_{0.1}(t)$ increases [see Eq. (5)]. Here, $B_{0.1}(t)$ is the downstream field amplified after the shock crossing, as described in Eq. (1). Thus, in the early phase of the Chandra observations (approximately 2000) or earlier, $t_{\rm cool}$ was much greater: from Eq. (5), $\epsilon_{\rm keV}=5$ at $B_{0.1}=1$ yields $t_{\rm cool}=25$ yr, comparable to $\tau^*$. On the other hand, electrons need time to be accelerated up to the TeV before cooling on the $t_{\rm cool}$ scale. As a result, an early-on cooling will not affect the electrons' spectrum.

*Discussion.*—We have presented the first quantitative theoretical model based on ideal MHD and small-scale dynamo downstream of shocks to explain the x-ray flux increase at a Cassiopeia A inward shock. We have provided an argument based on the ratio of cooling and acceleration times in support of the observed flux decrease. It is natural to inquire whether $t_{\rm cool}$ exceeds $t_{\rm acc}$ during the flux increase, as one could expect. By using the values observed or inferred ($r=3.8$, $\epsilon_{\rm keV}=5$, $C_{r,3}=6.5$, and $k_0=4.7$) and determined from our best fit of the flux increase ($B_{0(0.1)}=2.5$), the ratio of Eq. (6) to Eq. (5) leads to $t_{\rm acc}/t_{\rm cool}>1$ also prior to 2009, at odds with expectations. This should not be surprising, as current values of the observables are used that can lead to a significant overestimate of $t_{\rm acc}$ in the flux increase phase, as discussed below.

The use of $t_{\rm acc}/t_{\rm cool}$ as the criterion to determine the flux variability requires further discussion. The determination of $t_{\rm acc}$ is very sensitive to $k_0\propto C_r^2/E_{\gamma,{\rm cut,keV}}$, where $E_{\gamma,{\rm cut,keV}}$ is the electron cutoff energy [see Eq. (3) in Ref. [5] or Eq. (5) in Ref. [4]]. However, the uncertainty on $E_{\gamma,{\rm cut,keV}}$ alone dominated by the coarse spatial resolution of NuSTAR seems insufficient to justify the large ratio $t_{\rm acc}/t_{\rm cool}$. Grefenstette *et al.* [26] report $E_{\gamma,{\rm cut,keV}}\simeq 1.3$ keV (or $E_{\gamma,{\rm cut,keV}}\simeq 2.3$ keV) for the reverse (or forward) shock region, whereas an unlikely larger value ($E_{\gamma,{\rm cut,keV}}\simeq$ 10 keV) with other parameters unchanged would be required to satisfy the condition $t_{\rm acc}/t_{\rm cool}<1$.

Speculative arguments to justify $t_{\rm acc}/t_{\rm cool}>1$ during the flux increase involve also a temporal variation of the fitting parameters that have been assumed constant throughout this work and in Ref. [5]. For instance, the shock speed $C_r$ in the acceleration region likely decreased during the collision with the overdensity. At constant $k_0$, the relation $k_0\propto C_r^2/E_{\gamma,{\rm cut,keV}}$ implies that a greater $C_r$ would reduce $t_{\rm acc}$ [Eq. (6)], with $t_{\rm cool}$ unchanged only by requiring a greater $E_{\gamma,{\rm cut,keV}}$. On the other hand, $k_0$ might vary in time due to the growth of the magnetic turbulence and approach unity from above (below) for a quasiparallel (quasiperpendicular) magnetic topology [22]. So far, we have considered values of $k_0>1$. However, an intrinsic value $k_0<1$ or $k_0\ll 1$ in a region magnetically connected with the Chandra nonthermal bright inward shock could also lead to a production of TeV electrons that would migrate a short distance before cooling by synchrotron radiation; such a $k_0\ll 1$ would also enable a $t_{\rm acc}<t_{\rm cool}$. At present, we cannot disprove either magnetic topology. Thus, the observational uncertainties cannot rule out $t_{\rm acc}/t_{\rm cool}<1$ during the flux increase.

The flux decrease could have a different origin: the damping of the turbulent $B$ field downstream of the inward shock, e.g., due to nonlinear wave interactions [27], instead of energy losses of radiating electrons. The resulting flux decrease is expected to be achromatic from the radio to the hard x-ray spectrum. We will investigate such an effect in a forthcoming work. Another possible origin of the flux decrease is that the overdensity begins to disrupt at the $\nu F_\nu^{[4.2-6]\ {\rm keV}}$ peak, as $\tau^*\sim\ell_F/C_r$ is not negligible as compared to the shock crossing time $\sim R_c/C_r$. This effect will be accounted for in future numerical simulations.

We note that two more alternative scenarios for the inward shock location are suggested by Sato *et al.* [5] to explain the nonthermal emission, i.e., propagation through the unshocked ejecta or through the shocked layer with ion temperature ~46 keV, out of equilibrium with electrons. In both scenarios, Eq. (1) would result in $t_{\rm acc}/t_{\rm cool}<1$ throughout, at odds with the flux decrease. Moreover, in the latter scenario, the best-fit parameters are consistent with those in the case of ions in equilibrium with electrons at ~2 keV: $R_c=(1.21\pm 0.19)\times 10^{18}$ cm, $\ell_F=(7.30\pm 0.72)\times 10^{17}$ cm. However, the smaller compression ($r\sim 2.1$) would steepen the electron spectrum ($p\sim 4$), making it unlikely to accelerate up to ~10 TeV to produce the observed x rays. The former scenario would require the presence of a second molecular cloud in the unshocked ejecta beside the outer cloud that generates the inward shock. The $^{12}$CO maps from the Heinrich Hertz Submillimeter Telescope [5] with velocity $\simeq -40$ km/s reveal molecular clouds overlapping, in projection, to the innermost parts of the remnant, within the putative position of the reverse shock. In this case, the relative speed of the inward shock colliding with the second cloud in region W3 would be $C_r\simeq 3500$ km/s (see Ref. [5], Table 3). A value $\ell_F\simeq 3\times 10^{17}$ cm with unchanged $R_c$ would still lead to $\tau^*\simeq\ell_F/C_r\simeq 29$ yr. However, the observations do not allow us to clearly single out such a molecular cloud; thus, we do not consider such a scenario.

*Conclusion.*—We have shown that the x-ray flux increase between years 2000 and 2009 in a small region in the west limb of Cassiopeia A can trace the enhancement of the magnetic field due to vortical amplification as formerly proposed. The scaling of the saturation value $B/B_0$ with the Alfvén Mach number in the upstream fluid $M_A=C_r/v_A$ is simply given [7] by $B/B_0\sim M_A$. The low speed of the inward shock in the hot ejecta and the high value of $B_0$ jointly lead to a relatively low $M_A$, i.e.,

$M_A \simeq 3.8$ for a reasonable value of thermal proton density $n$ ($n = 0.1\ \mathrm{cm}^{-3}$ leads to $v_A = 1700$ km/s); thus, only a modest field amplification can be observed. The values of the diffusion coefficient departing from the Bohm limit that indicate relatively weak turbulence around the shock are also consistent with the inferred modest field amplification. We have provided a qualitative argument but not a firm theoretical model for the flux decrease between years 2009 and 2014. Further analysis is warranted and high-resolution follow-up monitoring of the region $W3$ is encouraged. This work demonstrates for the first time that the unfolding of a dynamo process formerly theoretically identified can be not only investigated in laboratory plasma astrophysics but also observed in astrophysical systems.

We thank the referees for useful feedback. F. F. acknowledges very helpful discussions with J. Raymond. The work of F. F. was supported in part by NASA under Grant No. NNX15AJ71G. F. F. also acknowledges support from Smithsonian Institution Scholarly Studies Grant No. 40488100HH00181. This work was partially supported by the Japan Society for the Promotion of Science KAKENHI Grant No. 16K17673 and No. 17H02864 (S. K.) and partially by Leading Initiative for Excellent Young Researchers, MEXT, Japan. T. S. is supported by the Special Postdoctoral Researchers Program in RIKEN.

[*]federico.fraschetti@cfa.harvard.edu

[1] S. P. Reynolds, Supernova remnants at high energy, Annu. Rev. Astron. Astrophys. **46**, 89 (2008).

[2] J. Meinecke *et al.*, Turbulent amplification of magnetic fields in laboratory laser-produced shock waves, Nat. Phys. **10**, 520 (2014).

[3] Y. Uchiyama and F. A. Aharonian, Fast variability of nonthermal x-ray emission in Cassiopeia A: Probing electron acceleration in reverse-shocked ejecta, Astrophys. J. Lett. **677**, L105 (2008).

[4] D. J. Patnaude, J. Vink, J. M. Laming, and R. A. Fesen, A decline in the nonthermal x-ray emission from Cassiopeia A, Astrophys. J. Lett. **729**, L28 (2011).

[5] T. Sato, S. Katsuda, M. Morii, A. Bamba, J. P. Hughes, Y. Maeda, M. Ishida, and F. Fraschetti, X-ray measurements of the particle acceleration properties at inward shocks in Cassiopeia A, Astrophys. J. **853**, 46 (2018).

[6] A. G. Sgro, The collision of a strong shock with a gas cloud—A model for Cassiopeia A, Astrophys. J. **197**, 621 (1975).

[7] F. Fraschetti, Turbulent amplification of a magnetic field driven by the dynamo effect at rippled shocks, Astrophys. J. **770**, 84 (2013).

[8] J. Giacalone and J. R. Jokipii, Magnetic field amplification by shocks in turbulent fluids, Astrophys. J. Lett. **663**, L41 (2007).

[9] T. Inoue, R. Yamazaki, S.-i. Inutsuka, and Y. Fukui, Toward understanding the cosmic-ray acceleration at young supernova remnants interacting with interstellar clouds: Possible applications to RX J1713.7-3946, Astrophys. J. **744**, 71 (2012).

[10] B. Müller, T. Melson, A. Heger, and H.-T. Janka, Supernova simulations from a 3D progenitor model—Impact of perturbations and evolution of explosion properties, Mon. Not. R. Astron. Soc. **472**, 491 (2017).

[11] R. A. Chevalier, J. M. Blondin, and R. T. Emmering, Hydrodynamic instabilities in supernova remnants—Self-similar driven waves, Astrophys. J. **392**, 118 (1992).

[12] J. M. Blondin and D. C. Ellison, Rayleigh-Taylor instabilities in young supernova remnants undergoing efficient particle acceleration, Astrophys. J. **560**, 244 (2001).

[13] F. Fraschetti, R. Teyssier, J. Ballet, and A. Decourchelle, Simulation of the growth of the 3D Rayleigh-Taylor instability in supernova remnants using an expanding reference frame, Astron. Astrophys. **515**, A104 (2010).

[14] R. M. Kulsrud and S. W. Anderson, The spectrum of random magnetic fields in the mean field dynamo theory of the Galactic magnetic field, Astrophys. J. **396**, 606 (1992).

[15] F. Fraschetti and M. Pohl, Particle acceleration model for the broad-band baseline spectrum of the Crab nebula, Mon. Not. R. Astron. Soc. **471**, 4856 (2017).

[16] U. Hwang and J. M. Laming, A Chandra x-ray survey of ejecta in the Cassiopeia A supernova remnant, Astrophys. J. **746**, 130 (2012).

[17] J. S. Lazendic, D. Dewey, N. S. Schulz, and C. R. Canizares, The kinematic and plasma properties of x-ray knots in Cassiopeia A from the Chandra HETGS, Astrophys. J. **651**, 250 (2006).

[18] G. B. Field, Thermal instability, Astrophys. J. **142**, 531 (1965).

[19] M. C. Begelman and C. F. McKee, Global effects of thermal conduction on two-phase media, Astrophys. J. **358**, 375 (1990).

[20] Y. Uchiyama, F. A. Aharonian, T. Tanaka, T. Takahashi, and Y. Maeda, Extremely fast acceleration of cosmic rays in a supernova remnant, Nature (London) **449**, 576 (2007).

[21] E. Parizot, A. Marcowith, J. Ballet, and Y. A. Gallant, Observational constraints on energetic particle diffusion in young supernovae remnants: Amplified magnetic field and maximum energy, Astron. Astrophys. **453**, 387 (2006).

[22] F. Fraschetti and J. Giacalone, Early-time velocity autocorrelation for charged particles diffusion and drift in static magnetic turbulence, Astrophys. J. **755**, 114 (2012).

[23] Likewise, in Ref. [5], the typical values are $t_{\mathrm{cool}} \sim 4$ yr and $t_{\mathrm{acc}} \sim 7$ yr with a constant $B$ field, and again $t_{\mathrm{acc}} > t_{\mathrm{cool}}$.

[24] J. Giacalone, Cosmic-ray transport and interaction with shocks, Space Sci. Rev. **176**, 73 (2013).

[25] F. Fraschetti and J. R. Jokipii, Time-dependent perpendicular transport of fast charged particles in a turbulent magnetic field, Astrophys. J. **734**, 83 (2011).

[26] B. W. Grefenstette, S. P. Reynolds, F. A. Harrison, T. B. Humensky, S. E. Boggs, C. L. Fryer, T. DeLaney, K. K. Madsen, H. Miyasaka, D. R. Wik, A. Zoglauer, K. Forster, T. Kitaguchi, L. Lopez, M. Nynka, F. E. Christensen, W. W. Craig, C. J. Hailey, D. Stern, and W. W. Zhang, Locating the most energetic electrons in Cassiopeia A, Astrophys. J. **802**, 15 (2015).

[27] M. Pohl, H. Yan, and A. Lazarian, Magnetically limited x-ray filaments in young supernova remnants, Astrophys. J. Lett. **626**, L101 (2005).